Density Functional Theory Study on the Complete Substitutions of Nd and Fe by Other Rare-earth and Transition-metal Elements in $Nd_2Fe_{14}B$ Compound①

RAO Shuang[a, b] LIN Chen-Sheng[b]
HE Zhang-Zhen[b] CHAI Guo-Liang[b②]

[a] (*College of Chemistry, Fuzhou University, Fuzhou* 350108, *China*)

[b] (*State Key Laboratory of Structural Chemistry, Fujian Institute of Research on the Structure of Matter, Chinese Academy of Sciences* (*CAS*), *Fuzhou* 350002, *China*)

ABSTRACT To search for proper alternatives to improve the magnetic properties of $Nd_2Fe_{14}B$, using first-principles density functional theory calculations we have systematically studied the $R_2M_{14}B$ (R = lanthanides from La to Lu; M = Mn, Fe, Co, and Ni) compounds with the isomorphic structure of $Nd_2Fe_{14}B$. The results show that for rare-earth elements, Pr is the most suitable choice for considering as an alternative of Nd. As for the substitution of Fe in $Nd_2Fe_{14}B$ by other transition-metal elements, Co is much more suitable than Mn and Ni because the latter two result in too significant reduction of the magnetic moment.

Keywords: permanent magnet materials, $Nd_2Fe_{14}B$, density functional theory calculations;
DOI: 10.14102/j.cnki.0254–5861.2011–2790

1 INTRODUCTION

$Nd_2Fe_{14}B$, the third-generation of rare-earth permanent magnet material, is the most widely used one in contemporary magnet[1, 2]. As a key component, $Nd_2Fe_{14}B$ frequently appears in the control system of inverter air conditioner, wireless communication system and other fields[3]. Global demand for high-performance $Nd_2Fe_{14}B$ has been growing rapidly[4]. Although rare-earth resources are abundant in China, it is hard to mine high-performance $Nd_2Fe_{14}B$ and ensure the utilization and recovery[4, 5]. Considering the atomic radius and similar chemical properties of adjacent chemical elements, many efforts have been done in order to search for a substitute for Nd–Fe–B by completely replacing Nd with other rare-earth elements or Fe with other metal elements or non-metal elements.

The substitution of Fe in $Nd_2Fe_{14}B$ and $Nd_2Fe_{14}C$ by other transition metal elements such as Mn, Co, and Ni has been extensively studied. For instance, in the study of $Nd_2Fe_{14-x}M_xB$ it is found that the partial substitution of Fe by Ni (Mn and Co) results in an increase (decrease) of lattice constant *c* and that Co (Mn) substitution in $Nd_2Fe_{14-x}M_xB$ results in an increase (decrease) of magnetization[6-8]. Similarly, in $Nd_2Fe_{14-x}M_xC$ system the Co and Ni (Mn) substitution for Fe can lead to an increase (decrease) of Curie temperature[9]. There are six distinct sites of Fe and two different sites of Nd in $Nd_2Fe_{14}B$ system, which are Fe(16*k*1), Fe(16*k*2), Fe(8*j*1), Fe(8*j*2), Fe(4*c*), Fe(4*e*), Nd(4*g*) and Nd(4*f*)[10]. The preference of substitution site has also been studied in $Nd_2Fe_{14-x}M_xB$. In the case of Si, Ge and Sn considered for M, they prefer to occupy the Fe(4*c*) site. Meanwhile, they lead to a reduction of volume and little change of magnetic moments of Fe atoms[11]. However, in the case of Ti or Nb considered for M, the most energetically favorable substitution site is the Fe(8*j*2) site[12, 13]. The replacement of Nd in $Nd_2Fe_{14}B$ by other rare earth elements has also been studied recently. It is found that Ce prefers to the Nd-4*g* site irrespective of the doping concentration[10]. La prefers to the Nd-4*f* (4*g*) site in low (high) doping concentration, while Pr behaves just in the opposite way to

Received 28 February 2020; accepted 4 April 2020

① This project was supported by the National Natural Science Foundation of China (No. 21703248), the Strategic Priority Research Program of the Chinese Academy of Sciences (No. XDB20000000), and the STS program under cooperative agreement between Fujian Province and Chinese Academy of Sciences (No 2017T3004)

② Corresponding author. Chai Guo-Liang. E-mail: g.chai@fjirsm.ac.cn

La[10, 14]. The systematical study on the substitution of Fe and Nd in $Nd_2Fe_{14}B$ was rarely performed in literature, which is of great importance to screen the proper substitution elements for improving the magnetic properties (i.e., magnetization, Curie temperature, and coercivity) of $Nd_2Fe_{14}B$.

In order to search for possible substitution elements for Nd and Fe in $Nd_2Fe_{14}B$, we have performed the first-principles calculations within generalized gradient approximation (GGA) to systematically study the $R_2M_{14}B$ (R = lanthanides from La to Lu; M = Mn, Fe, Co, and Ni) compounds with the isomorphic structure of $Nd_2Fe_{14}B$. In this work, we concentrated on the effect of R and M substitution on the lattice parameters and magnetic moments of $R_2M_{14}B$. Meanwhile we also checked the stability of $R_2M_{14}B$ by analyzing the calculated cohesive energy.

2 COMPUTATIONAL DETAILS

To understand the influence of rare-earth and transition metal elements substitution on the magnetic properties of $Nd_2Fe_{14}B$, we have performed the density functional theory (DFT) calculations on a series of compounds $R_2M_{14}B$ (R represents lanthanides from La to Lu, and M = Mn, Fe, Co, and Ni). The DFT calculations on $R_2M_{14}B$ were carried out using Vienna *ab-initio* simulation package (VASP) code[15, 16]. The ion-electron interaction was described by the projector-augmented wave (PAW) method[17]. The recommended standard PAW potentials in the VASP code were chosen for the lanthanides, transition metal, and boron atoms. The open-core (OC) PAW potentials were particularly used for Ce-Lu, where 4*f* electrons were treated as spin-polarized core electrons. The electron wavefunction was expanded by the plane wave basis set with an energy cutoff set to 400 eV after we investigated the literature and tested some values[18]. The exchange-correlation interaction was treated within the spin-polarized generalized gradient approximation (GGA) and the Perdew-Becke-Ernzerhof (PBE) exchange correlation functional was used[19]. The Brillouin zone integration was approximated by the Monkhorst-Pack k-point sampling method and a *k*-grid of 5 × 5 × 4 was employed[20]. Convergence criteria for the structure relaxation were set to 10^{-6} eV and 0.01 eV/Å for the energies and forces, respectively. The experimental lattice constants of $Nd_2Fe_{14}B$ are $a = b = 8.812$ Å and $c = 12.215$ Å[21]. Based on the experimental data, the lattice parameters and atomic positions were entirely relaxed by conjugate gradient algorithm.

Here we first obtained the spin moments of valence electrons of $R_2M_{14}B$ compounds from the self-consistent field (SCF) collinear spin-polarized calculations without spin-orbit coupling (SOC) for their relaxed crystal structures. Because the previous DFT calculations with SOC on $Nd_2Fe_{14}B$ showed that the orbital moments of Fe atoms in $Nd_2Fe_{14}B$ are the order of magnitude of 0.04 μ_B/atom[10, 14], we ignored the orbital moments of transition metal atoms in $R_2M_{14}B$ compounds. Based on the ionic model[22-24], the orbital moments of 4*f* electrons of each rare-earth atom in $R_2M_{14}B$ compounds were approximated as g_JJ, where g_J is the Landé *g*-factor and *J* is the total angular moment of 4*f* electrons of rare-earth elements, as given by Hund's rule. This is because the average magnetic moment per R atom in $R_2Fe_{14}B$ (R = Pr, Nd, Sm, Gd, Tb, Dy, Ho, Er, Tm, and Yb) estimated from the 4 K magnetization data is very close to the magnetic moment g_JJ of the corresponding trivalent R ions[24]. For the less (more) than half-filled 4*f* electron shell of rare-earth elements, its orbital moment aligns parallel (antiparallel) to the spin moment of 3*d* electrons of transition metal atoms in $R_2M_{14}B$[23, 25]. The total magnetic moments of $R_2M_{14}B$ compounds were estimated from the spin moments of valence electrons and the approximated orbital moments of rear-earth 4*f* electrons. We should point out that this approximation does not take into account the contribution from the orbital moments of transition metal atoms and the SOC. Such an approximation has been employed in literature[26-28] to estimate the magnetic moments of $NdFe_{11}Ti$, $Nd_2Fe_{14}B$, and RFe_{12}. The obtained magnetic moment of $Nd_2Fe_{14}B$ is in good agreement with the experiment value[27]. The reliability of the open-core treatment for the rear-earth atoms in $Nd_2Fe_{14}B$ has been discussed in literature, *e.g.*, in Ref.[27], and it was found that the magnetic moment of $Nd_2Fe_{14}B$ calculated with GGA+OC and GGA+U shows the same tendency.

3 RESULTS AND DISCUSSION

3. 1 Crystal structure

The neutron powder diffraction analysis and single-crystal X-ray diffraction experiments showed that $Nd_2Fe_{14}B$ crystallizes in the tetragonal $CaCu_5$-type structure with space group *P*42/*mnm*. Each crystallographic unit cell contains four chemical formula units, namely 68 atoms. The $Nd_2Fe_{14}B$ crystallographic unit cell is depicted in Fig. 1, where the symmetry-inequivalent sites of atoms (*i.e.*, Wyckoff positions) are labelled. The Nd atoms occupy two different sites, 4*f* and

4*g*. The Fe atoms contain six distinct sites of 4*c*, 4*e*, 8*j*1, 8*j*2, 16*k*1, and 16*k*2. The nonmetal element boron (B) lies in 4*g* site. The total magnetic moment of $Nd_2Fe_{14}B$ reported in experiments is 37.1 μ_B/formula unit (f.u.)[29]. The lattice constants of $Nd_2Fe_{14}B$ obtained from the X-ray diffraction data are $a = b = 8.812$ Å and $c = 12.215$ Å[21]. The calculated values of lattice constants (a, c) of $Nd_2Fe_{14}B$ are presented in Table 1: $a = 8.7518$ Å and $c = 12.1082$ Å. We can see that the difference between the theoretically predicted and experimentally measured values for the lattice constants of $Nd_2Fe_{14}B$ is less than 1%. Therefore, the calculated results are in good agreement with the available experimental values, indicating that the present calculation setup is good enough to study the structure and magnetic properties of $R_2M_{14}B$.

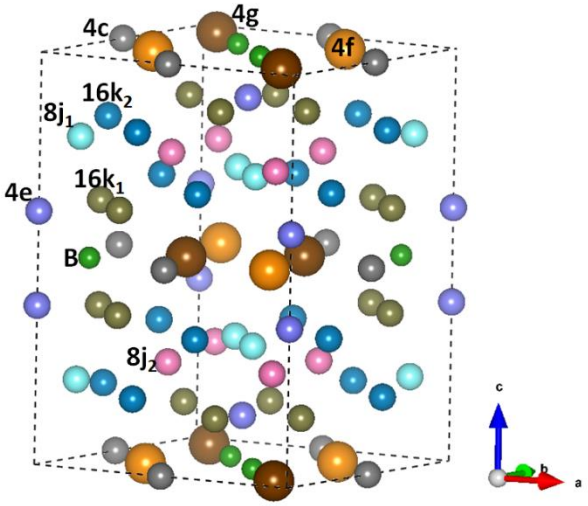

Fig. 1. Schematic drawing of crystal structure of $Nd_2Fe_{14}B$. Nd atoms occupy two distinct symmetry sites: 4*g* (*x*, –*x*, 0) and 4*f* (*x*, *x*, 0). Fe atoms occupy six different symmetry sites: 4*c* (0, 1/2, 0), 4*e* (0, 0, *z*), 8*j*1 (*x*, *x*, *z*), 8*j*2, 16*k*1 (*x*, *y*, *z*), and 16*k*2. B atoms occupy one symmetry site: 4*g*

Table 1. Calculated Lattice Constants (a and c, in Å) of $R_2Fe_{14}B$ Compounds, where R Represents the Lanthanide Elements from La to Lu

Compound	Calculated	Experimental
	(a, c)	(a, c)
$La_2Fe_{14}B$	(8.7611, 12.2370)	(8.822, 12.338)[21]
$Ce_2Fe_{14}B$	(8.7708, 12.2271)	(8.778, 12.094)[34]
$Pr_2Fe_{14}B$	(8.7614, 12.1625)	(8.82, 12.25)[35]
$Nd_2Fe_{14}B$	(8.7518, 12.1082)	(8.812, 12.215)[36]
$Pm_2Fe_{14}B$	(8.7417, 12.0618)	
$Sm_2Fe_{14}B$	(8.7346, 12.0262)	(8.82, 11.94)[37]
$Eu_2Fe_{14}B$	(8.7264, 11.9856)	
$Gd_2Fe_{14}B$	(8.7167, 11.9508)	(8.79, 12.074)[38]
$Tb_2Fe_{14}B$	(8.7093, 11.9199)	(8.77, 12.05)[39]
$Dy_2Fe_{14}B$	(8.7032, 11.8914)	(8.76, 11.99)[37]
$Ho_2Fe_{14}B$	(8.6963, 11.8628)	(8.75, 11.99)[37]
$Er_2Fe_{14}B$	(8.6894, 11.8346)	(8.75, 11.99)[37]
$Tm_2Fe_{14}B$	(8.6839, 11.8079)	(8.74, 11.94)[37]
$Yb_2Fe_{14}B$	(8.6780, 11.7815)	(8.74, 11.92)[1]
$Lu_2Fe_{14}B$	(8.6724, 11.7554)	(8.693, 11.911)[40]

Table 1 lists the calculated lattice constants of $R_2Fe_{14}B$ along a comparison with the available experiment results. Table S1 of Supplementary Information lists the calculated lattice constants a and c of $R_2Mn_{14}B$, $R_2Co_{14}B$ and $R_2Ni_{14}B$. To make the comparison more transparent, the change of lattice constants of $R_2M_{14}B$ with respect to the rare-earth element R is illustrated in Fig. 2. For the lanthanides (R) from La to Lu, both lattice constants a and c of $R_2M_{14}B$ (M = Mn, Fe, Co, and Ni) have a tendency toward decrease. When the R changes from La to Lu, the reduction of lattice constant a of $R_2M_{14}B$ is less than that of c of $R_2M_{14}B$. For a given rare-earth element (R) in $R_2M_{14}B$, the change of c as the

transition metal element (M) is also more significant than that of *a*. Therefore, we can anticipate that the (partial) substitution of La, Ce, and Pr for Nd in $Nd_2Fe_{14}B$ would lead to a volume expansion for $Nd_2Fe_{14}B$, while the (partial) substitution of other lanthanides (namely from Pm to Lu) would cause a volume shrinkage. The (partial) substitution of Mn, Co, and Ni for Fe in $Nd_2Fe_{14}B$ would give rise to a volume shrinkage. Fig. 3 presents the calculated unit cell volumes (Ω) of $R_2M_{14}B$ compounds, which are also listed in Table S2 of Supplementary Information accordingly. As discussed above, the volume of $R_2M_{14}B$ increases from to La to Ce and then decreases from Ce to Lu in each case of M = Mn, Fe, Co and Ni. For each rare-earth element compound, the general trend is $\Omega(R_2Fe_{14}B) > \Omega(R_2Mn_{14}B) > \Omega(R_2Ni_{14}B) \approx \Omega(R_2Co_{14}B)$.

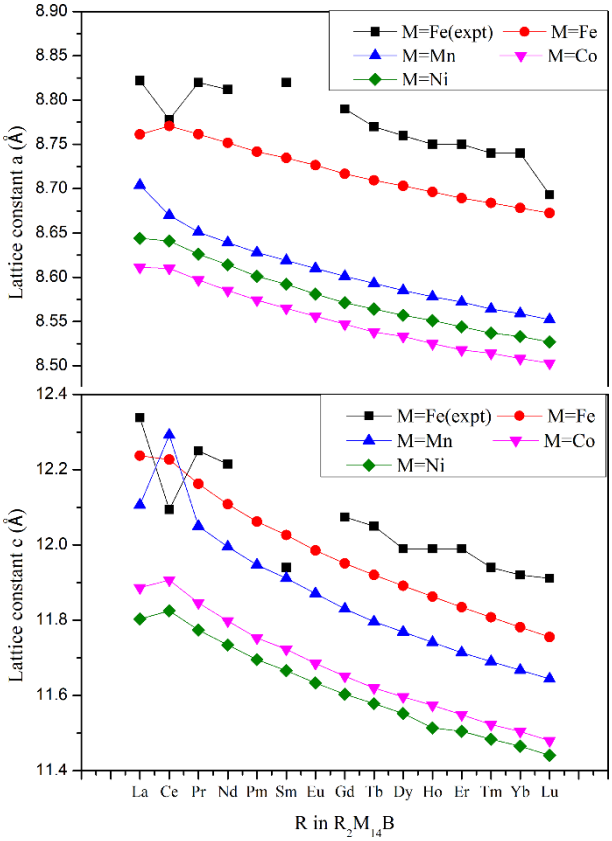

Fig. 2. Lattice constants (*a* and *c*, in Å) of $R_2M_{14}B$

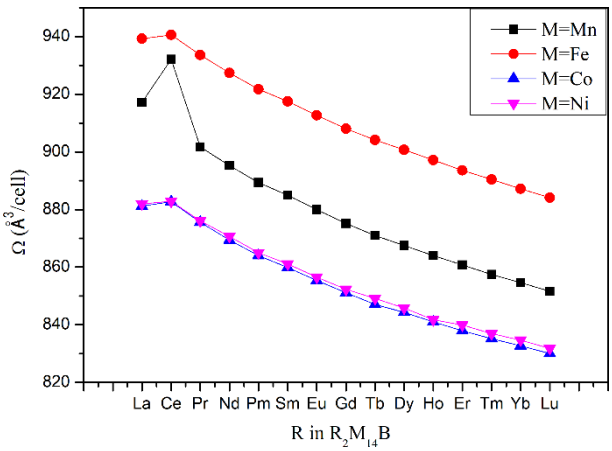

Fig. 3. Lattice volume (Ω, in Å^3/cell) of $R_2M_{14}B$

Lanthanide contraction refers to the shrinkage of atomic radius of lanthanide elements from La to Lu due to the shielding effect from 5*s*5*p* electrons on 4*f* electron. As the filled 4*f* electrons increase, more 4*f* electrons gather around

their nucleus unable to escape, making the atomic radius smaller[30]. When lanthanide element reacts with other elements and turns into trivalent ion, the trend of monotonic decreasing of ionic radii still exists from La^{3+} to Lu^{3+}. As a result, the monotonic decrease of lattice constant (*a*, *c*) and volume (Ω) in Figs. 2 and 3 can be attributed to the lanthanide contraction. In the case of $Ce_2M_{14}B$ compounds, Ce may not take the completely trivalent state, but it is somewhere between trivalent and tetravalent. Some 4*f* electrons of Ce in its own compound are localized and cannot get bonding, while others react with transition metals M and B[31, 32].

3. 2 Magnetic moments

As already mentioned in the above section of computational method, the following approximations were taken to calculate the total magnetic moments of $R_2M_{14}B$. First, the magnetic moments of R and M atoms are collinear. Second, the total magnetic moment of R includes both the spin and orbital magnetic moments. The orbital moment of M atom is ignored because the orbital moments of Fe atoms in $Nd_2Fe_{14}B$ are small, at the order of magnitude of 0.04 μ_B/atom, so that the magnetic moment of M atom includes only the contribution of valence electrons. Third, the orbital moment of 4*f* electrons of R atom in $R_2M_{14}B$ was approximated to the magnetic moment g_JJ of the corresponding trivalent R ion (R^{3+}), as shown in Table 2.

Table 2. Total Angular Momentum *J*, the Land´e g_J Factor, and Magnetic Moments g_JJ for the Trivalent Lanthanide Ions (R^{3+})[24, 25, 41]. The Average Magnetic Moment m_R Per R Atom in $R_2Fe_{14}B$ Compound was Estimated from the 4 K Magnetization Data[24]

R	*J*	g_J	g_JJ	m_R[24]
La	0		0.0	
Ce	2.5	6/7	2.143	
Pr	4.00	4/5	3.2	3.1
Nd	4.50	8/11	3.273	3.2
Pm	4.00	3/5	2.4	
Sm	2.50	2/7	0.714	1.0
Eu	0.00		0.0	
Gd	3.50	2	7.0	–6.8
Tb	6.00	3/2	9.0	–9.1
Dy	7.50	4/3	10.0	–10.1
Ho	8.00	5/4	10.0	–10.1
Er	7.50	6/5	9.0	–9.3
Tm	6.00	7/6	7.0	–6.7
Yb	3.50	8/7	4.0	–4.2
Lu	0.00		0.0	

To check the reliability of the present method used to study the magnetic moments of $R_2M_{14}B$, we first compare the obtained local magnetic moments of Fe atoms in $Nd_2Fe_{14}B$ and total magnetic moment of $Nd_2Fe_{14}B$ with the previous calculation results and the available experiment data, as shown in Table 3. Our calculation results are in good agreement with those obtained by Tatesu et al.[27] using the similar GGA+OC approach. The slight difference in the local magnetic moment of Fe atoms may be caused by the different radius size used in the estimation of local magnetic moments. The Fe-8*j*2(-4*e*) sites have the largest (smallest) local magnetic moments, which are consistent with the trend in the previous LDA/GGA+U+SOC calculation[10, 14] and experiment[33] results. The local magnetic moments of Fe atoms at the 16*k*1, 16*k*2 and 4*c* sites are underestimated by ~0.3 μ_B/atom with respect to the experiment results[33], which is caused partially by the ignored SOC between the Nd 4*f* and Fe 3*d* electrons and also by the ambiguity of radius size used in estimating the local magnetic moments. The obtained total magnetic moment of $Nd_2Fe_{14}B$ is about 37.63 μ_B/f.u. and in good agreement with the experimental value (37.1 μ_B/f.u.)[33]. Therefore, the present method is accurate enough to study the magnetic moments of $R_2M_{14}B$.

In $Nd_2Fe_{14}B$, we completely replace Nd with other 14 lanthanide elements to obtain $R_2Fe_{14}B$ series of compounds. At first, we pay attention to the total spin magnetic moments (denoted as μ_S) of $R_2Fe_{14}B$, which was obtained directly from the collinear spin-polarized calculations. The orbital magnetic moments of the 4*f* electrons of rare-earth atoms in $R_2Fe_{14}B$ were approximated to the magnetic moment g_JJ of the corresponding trivalent rare-earth ions based on the ionic model[22-24], as listed in Table 2. Among the 15 rare-earth

elements of lanthanide, the La and Lu have none orbital moments. The orbital magnetic moment of Eu is quenched completely to zero. When the number of electrons in the 4*f* electron shell is less than half for a rare-earth element, the total magnetic moment (denoted as μ_t) of $R_2M_{14}B$ is $\mu_t = \mu_S + g_J J(R)$; and more than half of the corresponding is $\mu_t = |\mu_S - g_J J(R)|$. The same way was done for the cases of $R_2Mn_{14}B$, $R_2Co_{14}B$ and $R_2Ni_{14}B$. The calculated results of total magnetic moments (μ_t) of $R_2M_{14}B$ are displayed in Fig. 4 and listed in Table S3 of Supplementary Information.

Table 3. Local Magnetic Moments of Fe Atoms (m_{Fe}, in μ_B) and Total Magnetic Moments (μ_t, in μ_B/f.u.) of $Nd_2Fe_{14}B$ Obtained by the Distinct Computational Methods. The Experimental Results are Listed for Comparison

Method		m_{Fe}						μ_t
		16*k*1	16*k*2	8*j*1	8*j*2	4*e*	4*c*	
This work	GGA+OC [a]	2.23	2.31	2.23	2.69	2.02	2.43	37.63
Ref. [27]	GGA+OC [b]	2.31	2.39	2.34	2.76	2.10	2.54	37.42
Ref. [10]	GGA+U [c]	2.ta25	2.33	2.18	2.61	2.19	2.41	
Ref. [10]	GGA+U+SOC [c]	2.48	2.45	2.25	2.78	2.13	2.65	
Ref. [14]	LDA+U [d]	2.19	2.26	2.12	2.66	1.99	2.35	36.89
Ref. [14]	LDA+U+SOC [d]	2.17	2.23	2.09	2.64	1.97	2.32	30.02
Expt. [33] [e]		2.60	2.60	2.30	2.85	2.10	2.75	37.1

[a] The PAW method with an open-core PAW potential used for Nd.

[b] The linear combination of pseudo-atomic-orbitals method with an open-core norm-conserving pseudopotential used for Nd.

[c] The PAW method with an effective U of 5.0 eV applied on the 4*f* electrons of Nd.

[d] The full potential linearized augmented plane wave method with an effective U of 6.0 eV applied on the 4*f* electrons of Nd.

[e] T = 4.2 K

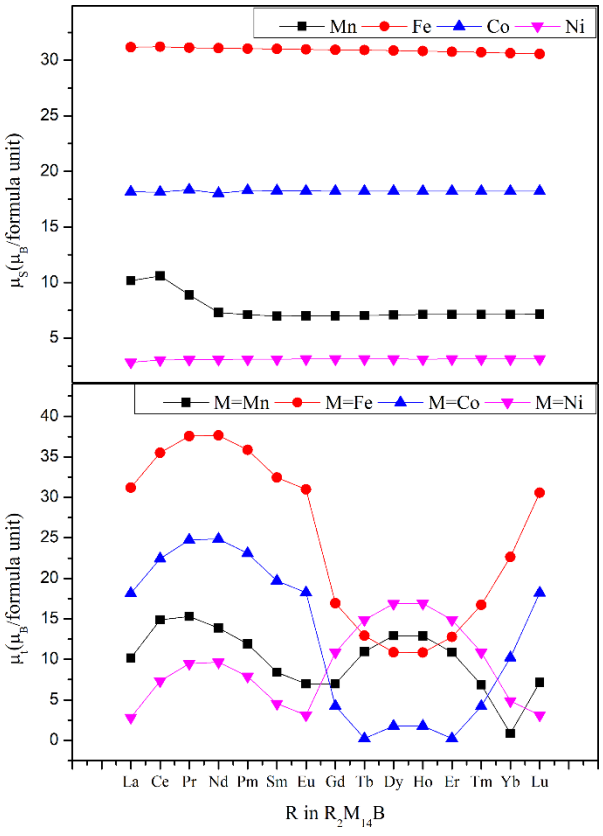

Fig. 4. Calculated spin magnetic moment (μ_S, in μ_B/f.u.) and total magnetic moment (μ_t, in μ_B/f.u.) of $R_2M_{14}B$

Now we look at the dependence of total magnetic moments of $R_2Fe_{14}B$ on the rare-earth elements. As the total spin magnetic moment of $R_2Fe_{14}B$ is almost around 31.0 μ_B, irrespective of the different rare-earth elements, the change in total magnetic moments $R_2Fe_{14}B$ follows the trend in the orbital moments of the 4*f* electrons of R atoms. For the same transition metal, the magnetic moments of $Pr_2M_{14}B$ and $Nd_2M_{14}B$ are almost the same. Compared with the Fe and Co

series ($R_2Fe_{14}B$ and $R_2Co_{14}B$), the spin magnetic moments of the Mn and Ni series ($R_2Mn_{14}B$ and $R_2Ni_{14}B$) are too small. For the light rare-earth elements with less than a half-filled 4*f* electron shell, the order of total magnetic moments is $\mu_t(R_2Fe_{14}B) > \mu_t(R_2Co_{14}B) > \mu_t(R_2Mn_{14}B) > \mu_t(R_2Ni_{14}B)$. For the heavy rare-earth elements with more than a half-filled 4*f* electron shell, their 4*f* orbital magnetic moments are antiparallel to the spin magnetic moments of transitional metal 3*d* electrons, and thus the corresponding total magnetic moments of $R_2M_{14}B$ are significantly reduced with respect to that of $Nd_2Fe_{14}B$. From this aspect, the substitution of Nd by other light rare-earth elements is more favorable to maintain the magnetic properties of $Nd_2Fe_{14}B$. In the case of light rare-earth elements, the magnetic moment of $R_2Co_{14}B$ series is slightly smaller than those of $R_2Fe_{14}B$ systems so that it would be worthwhile to consider the incorporation of Co into $R_2Fe_{14}B$.

3. 3 Cohesive energy

The cohesive energy E_{coh} of a compound is defined as the energy difference between its total energy and the sum of the total energies of its constituent atoms. For $R_2M_{14}B$, its E_{coh} is calculated according to the following equation:

$$E_{coh} = E_{R2M14B} - 2E_R - 14E_M - E_B \quad (1)$$

where E_R, E_M, and E_B are the total energies of isolated rare-earth, transition metal, and boron atoms, respectively. E_{R2M14B} is the total energy of $R_2M_{14}B$. The more negative value of E_{coh} indicates that $R_2M_{14}B$ is more stable with respect to the corresponding constituent atoms.

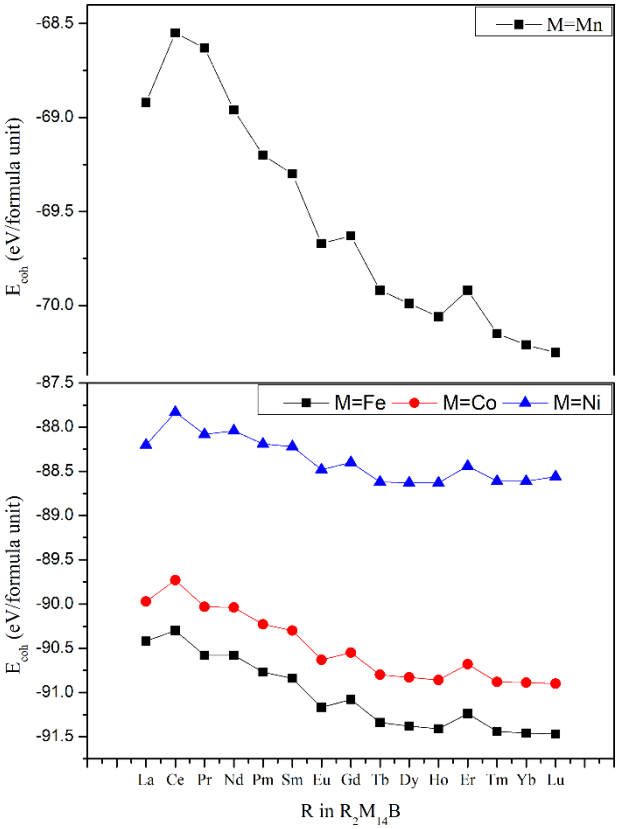

Fig. 5. Cohesive energy (E_{coh}, in eV/f.u.) of $R_2M_{14}B$

We present the calculated cohesive energies of $R_2M_{14}B$ in Fig. 5 and list them in Table S4 of Supplementary Information. For all lanthanide elements studied here, the general trend is that the cohesive energies of $R_2M_{14}B$ take an order of $R_2Mn_{14}B > R_2Ni_{14}B > R_2Co_{14}B > R_2Fe_{14}B$. It is remarkably noted that the cohesive energies of $R_2Mn_{14}B$ are much larger than those of $R_2Ni_{14}B$, between which the energy differences are around 19.5 eV/formula unit. However, the cohesive energies of $R_2Co_{14}B$ are very close to those of $R_2Fe_{14}B$, between which the energy differences are around 1.0 eV/formula unit. Therefore, the formation of $R_2Mn_{14}B$ would be thermodynamically unstable as compared with $R_2Ni_{14}B$, $R_2Co_{14}B$, and $R_2Fe_{14}B$. It also suggests that the incorporation of Mn into $R_2Fe_{14}B$ would be more energetically costly as compared with the incorporation of Ni and Co into $R_2Fe_{14}B$. On the other hand, the Co substitution for Fe in $R_2Fe_{14}B$ would be more thermodynamically favorable than the Ni and Mn substitution. Now let us see the dependence of cohesive

energies of $R_2Fe_{14}B$ on the rare-earth elements. If taking the cohesive energy of $Nd_2Fe_{14}B$ as a reference, the relative energy differences in the cohesive energies of other $R_2Fe_{14}B$ ($R \neq Nd$) are in a $-0.90 \sim 0.28$ eV/formula unit range. Therefore, the substitution of Nd by other lanthanide elements would be thermodynamically favorable. Indeed, many compounds of $R_2Fe_{14}B$ serials have been synthesized in experiment, as listed in Table 1.

4 CONCLUSION

To search for an alternative for $Nd_2Fe_{14}B$, we have studied the substitution of other rare-earth elements for Nd along with transition elements Mn, Co and Ni for Fe, which implies sixty compounds. Within the framework of density functional theory, we optimized the crystal structures and calculated the magnetic moments and cohesion energies of these sixty compounds, finding that the substitution leads to small changes in both lattice constants and volumes of these candidates with respect to those of $Nd_2Fe_{14}B$. For the rare-earth elements, Pr is the most possible nominee to Nd. As for transition-metal elements, Co substitution manages with an effort to keep the magnetic moments, while Mn and Ni substitutions make the magnetic moments of $Nd_2Fe_{14}B$ too small to be considered. For transition-metal substitutions, the most suitable choice for Fe is Co, followed by Ni, while the Mn substitution is thermodynamically unfavorable with a serious disadvantage, namely a significant reduction of magnetic moments. Therefore, the incorporation of Mn into $Nd_2Fe_{14}B$ shall not be considered. In this proposition of complete replacing for $Nd_2Fe_{14}B$, it might be better to consider $Pr_2Fe_{14}B$. In addition, although $Pr_2Fe_{14}B$ and $Nd_2Fe_{14}B$ have similar amount of total magnetic moments, further comparisons need to be made from mining cost and magneto-crystalline anisotropy, which will be studied in our future work. Furthermore, the complete substitution may be thermodynamically unfavorable in many cases for $Nd_2Fe_{14}B$, so we will consider the partial substitution as well as doping some other elements in the next step.

REFERENCES

(1) Sagawa, M.; Yamamoto, H.; Fujimura, S.; Matsuura, Y. Nd-Fe-B permanent magnet materials. *Jpn. J. Appl. Phys.* **1987**, 26, 785–800.

(2) Pan, S. *Rare Earth Permanent-Magnet Alloys' High Temperature Phase Transformation*. Springer, Berlin Heidelberg **2013**, p129–150.

(3) Honshima, M.; Ohashi, K. High-energy NdFeB magnets and their applications. *J. Mater. Eng. Perform.* **1994**, 3, 218–222.

(4) Zhou, X.; Tian, Y. L.; Yu, H. Y.; Zhang, H.; Zhong, X. C.; Liu, Z. W. Synthesis of hard magnetic NdFeB composite particles by recycling the waste using microwave assisted auto-combustion and reduction method. *Waste. Manage.* **2019**, 87, 645–651.

(5) Du, X.; Graedel, T. E. Global rare earth in-use stocks in NdFeB permanent magnets. *J. Ind. Ecol.* **2011**, 15, 836–843.

(6) Abache, C.; Oesterreicher, H. Structural and magnetic properties of $R_2Fe_{14-x}T_xB$ (R = Nd, Y; T = Cr, Mn, Co, Ni, Al). *J. Appl. Phys.* **1986**, 60, 1114–1117.

(7) Bolzoni, F.; Leccabue, F.; Moze, O.; Pareti, L.; Solzi, M. Magnetocrystalline anisotropy of Ni and Mn substituted $Nd_2Fe_{14}B$ compounds. *J. Magn. Magn. Mater.* **1987**, 67, 373–377.

(8) Doi, M.; Matsui, M. Substitution effect of Fe sites in $Nd_2Fe_{14}B$. *IEEE Translat. J. Magn. Jpn.* **1992**, 7, 38–44.

(9) Kappel, W.; Burzo, E.; Pop, V. Magnetic properties of $Nd_2Fe_{14-x}M_xC$ compounds. *J. Magn. Magn. Mater.* **1996**, 157–158, 35–36.

(10) Alam, A.; Khan, M.; McCallum, R. W.; Johnson, D. D. Site-preference and valency for rare-earth sites in $(R\text{-}Ce)_2Fe_{14}B$ magnets. *Appl. Phys. Lett.* **2013**, 102, 042402–4.

(11) Liu, X. B.; Liu, J. P.; Zhang, Q.; Altounian, Z. The Fe substitution in $Nd_2(Fe, M)_{14}B$ (M= Si, Ge and Sn): a first-principles study. *Comput. Mater. Sci.* **2014**, 85, 186–192.

(12) Dong, G.; Sui, Y.; Qian, P.; Wu, Y.; Guo, L. Experimental and theoretical studies on site preference of Ti in $Nd_2(Fe, Ti)_{14}B$. *J. Magn. Magn. Mater.* **2015**, 379, 108–111.

(13) Yang, F.; Guo, L.; Sui, Y.; Qian, P.; Guo, Z.; Li, P. Effect of Nb on magnetic properties, microstructures, and site preference in Nd–Fe–B nanograin single-phase alloy. *J. Supercond. Nov. Magn.* **2016**, 29, 2591–2597.

(14) Khan, I.; Hong, J. Site preferences for La and Pr in $Nd_2Fe_{14}B$ permanent magnet: a first principles study. *J. Korean Phys. Soc.* **2016**, 69, 1564–1570.

(15) Kresse, G.; Furthmuller, J. Efficiency of *ab-initio* total energy calculations for metals and semiconductors using a plane-wave basis set. *Comput. Mater. Sci.* **1996**, 6, 15–50.

(16) Kresse, G.; Furthmuller, J. Efficient iterative schemes for *ab initio* total-energy calculations using a plane-wave basis set. *Phys. Rev. B* **1996**, 54,

11169–11186.

(17) Kresse, G.; Joubert, D. From ultrasoft pseudopotentials to the projector augmented-wave method. *Phys. Rev. B* **1999**, 59, 1758–1775.

(18) Drebov, N.; Martinez-Limia, A.; Kunz, L.; Gola, A.; Shigematsu, T.; Eckl, T.; Gumbsch, P.; Elsässer, C. Ab initio screening methodology applied to the search for new permanent magnetic materials. *New. J. Phys.* **2013**, 15, 125023–24.

(19) Perdew, J. P.; Burke, K.; Ernzerhof, M. Generalized gradient approximation made simple. *Phys. Rev. Lett.* **1996**, 77, 3865–3868.

(20) Monkhorst, H. J.; Pack, J. D. Special points for Brillouin-zone integrations. *Phys. Rev. B* **1976**, 13, 5188–5192.

(21) Sinnema, S.; Radwanski, R. J.; Franse, J. J. M.; de Mooij, D.; Buschow, K. Magnetic properties of ternary rare-earth compounds of the type $R_2Fe_{14}B$. *J. Magn. Magn. Mater.* **1984**, 44, 333–341.

(22) Ashcroft, N. W.; Mermin, N. D. *Solid State Physics*. Saunders College, Philadelphia **1976**, p166–404.

(23) Söderlind, P.; Turchi, P. E. A.; Landa, A.; Lordi, V. Ground-state properties of rare-earth metals: an evaluation of density-functional theory. *J. Phys. Condens. Matter.* **2014**, 26, 416001–8.

(24) Herbst, J. F. $R_2Fe_{14}B$ materials: intrinsic properties and technological aspects. *Rev. Mod. Phys.* **1991**, 63, 819–898.

(25) Miyake, T.; Akai, H. Quantum theory of rare-earth magnets. *J. Phys. Soc. Jpn.* **2018**, 87, 041009–10.

(26) Harashima, Y.; Terakura, K.; Kino, H.; Ishibashi, S.; Miyake, T. Nitrogen as the best interstitial dopant among X = B, C, N, O, and F for strong permanent magnet $NdFe_{11}Ti_X$: first-principles study. *Phys. Rev. B* **2015**, 92, 184426–13.

(27) Tatetsu, Y.; Harashima, Y.; Miyake, T.; Gohda, Y. Role of typical elements in $Nd_2Fe_{14}X$ (X = B, C, N, O, F). *Phys. Rev. Mater.* **2018**, 2, 074410–9.

(28) Harashima, Y.; Fukazawa. T.; Kino, H.; Miyake, T. Effect of R-site substitution and the pressure on stability of RFe_{12}: a first-principles study. *J. Appl. Phys.* **2018**, 124, 163902–6.

(29) Givord, D.; Li, H. S.; De La Bâthie, R. P. Magnetic properties of $Y_2Fe_{14}B$ and $Nd_2Fe_{14}B$ single crystals. *Solid State Commun.* **1984**, 51, 857–860.

(30) Hughes, I. D.; Däne, M.; Ernst, A.; Hergert, W.; Lüders, W.; Poulter, J.; Staunton, J. B.; Svane, A.; Szotek, Z.; Temmerman, W. M. Lanthanide contraction and magnetism in the heavy rare earth elements. *Nature* **2007**, 446, 650–653.

(31) Wang, J.; Liang, L.; Zhang, L. T.; Yano, M.; Terashima, K.; Kada, H.; Kato, S.; Kadono, T.; Imada, S.; Nakamura, T.; Hirano, S. Mixed-valence state of Ce and its individual atomic moments in $Ce_2Fe_{14}B$ studied by soft X-ray magnetic circular dichroism. *Intermetallics* **2016**, 69, 42–46.

(32) Li, Y. Y.; Cheng, W. D.; Zhang, H.; Lin, C. S.; Zhang, W. L.; Geng, L.; Chai, G. L.; Luo, Z. Z.; He, Z. Z. A series of novel rare-earth bismuth tungstate compounds $LnBiW_2O_9$ (Ln = Ce, Sm, Eu, Er): synthesis, crystal structure, optical and electronic properties. *Dalton Trans.* **2011**, 40, 7357–7364.

(33) Givord, D.; Li, H. S.; Tasset, F. Polarized neutron study of the compounds $Y_2Fe_{14}B$ and $Nd_2Fe_{14}B$. *J. Appl. Phys.* **1985**, 57, 4100–4102.

(34) Herbst, J. F.; Yelon, W. B. Crystal and magnetic structure of $Ce_2Fe_{14}B$ and $Lu_2Fe_{14}B$. *J. Magn. Magn. Mater.* **1986**, 54, 570–572.

(35) Sagawa, M.; Fujimura, S.; Yamamoto, H.; Matsuura, Y.; Hiraga, K. Permanent magnet materials based on the rare earth-iron-boron tetragonal compounds. *IEEE Trans. Magn.* **1984**, 20, 1584–1589.

(36) Yang, Y. C.; Zhang, X. D.; Kong, L. S.; Pan, Q.; Hou, Y. T.; Huang, S.; Yang, L.; Ge, S. L. Structural and magnetic properties of nitride compounds of the type $R_2Fe_{17}N_x$, $R_2Fe_{14}BN_x$ and $RTiFe_{11}N_x$. *J. Less Common. Met.* **1991**, 170, 37–44.

(37) Hirosawa, S.; Matsuura, Y.; Yamamoto, H.; Fujimura, S.; Sagawa, M.; Yamauchi, H. Magnetization and magnetic anisotropy of $R_2Fe_{14}B$ measured on single crystals. *J. Appl. Phys.* **1986**, 59, 873–879.

(38) Buschow, K. H. J.; De Mooij, D. B.; Daams, J. L. C. Phase relationships, magnetic and crystallographic properties of NdFeB alloys. *J. Less Common. Met.* **1986**, 115, 357–366.

(39) Sagawa, M. Structure and magnetic properties of Nd-Fe-B permanent magnet materials. *IEEE Translat. J. Magn. Jpn.* **1985**, 1, 62–65.

(40) Oesterreicher, H.; Spada. F.; Abache, C. Anisotropic and high magnetization rare earth transition metal compounds containing metalloids. *Mater. Res. Bull.* **1984**, 19, 1069–1076.

(41) Temmerman, W. M.; Petit, L.; Svane, A.; Szotek, Z.; Luders, M.; Strange, P.; Staunton, J.; Hughes, I.; Gyorffy, B. *The Dual, Localized or Band-like, Character of the 4f-States, in: Handbook on the Physics Chemistry of Rare Earths Volume 39*. Elsevier **2009**, p1–112.